THE JOURNAL OF BIOLOGICAL CHEMISTRY
Vol. 277, No. 44, Issue of November 1, pp. 41865–41871, 2002

Printed in U.S.A.

Electron Transfer from the Rieske Iron-Sulfur Protein (ISP) to Cytochrome *f in Vitro*

IS A GUIDED TRAJECTORY OF THE ISP NECESSARY FOR COMPETENT DOCKING?*

Received for publication, June 11, 2002, and in revised form, August 23, 2002
Published, JBC Papers in Press, August 30, 2002, DOI 10.1074/jbc.M205772200

Glenda M. Soriano‡§, Lian-Wang Guo¶, Catherine de Vitry‖, Toivo Kallas¶, and William A. Cramer‡§**

From the ‡Department of Biological Sciences and Program in Biochemistry/Molecular Biology, Purdue University, West Lafayette, Indiana 47907-1392, the ¶Department of Biology and Microbiology, University of Wisconsin, Oshkosh, Wisconsin 54901, and ‖Physiologie Membranaire et Moléculaire du Chloroplaste, CNRS UPR 1261, Institute de Biologie Physico-Chimique, 75005 Paris, France

The time course of electron transfer *in vitro* between soluble domains of the Rieske iron-sulfur protein (ISP) and cytochrome *f* subunits of the cytochrome b_6f complex of oxygenic photosynthesis was measured by stopped-flow mixing. The domains were derived from *Chlamydomonas reinhardtii* and expressed in *Escherichia coli*. The expressed 142-residue soluble ISP apoprotein was reconstituted with the [2Fe-2S] cluster. The second-order rate constant, $k_2^{(ISP\text{-}f)} = 1.5 \times 10^6$ M^{-1} s^{-1}, for ISP to cytochrome *f* electron transfer was $<10^{-2}$ of the rate constant at low ionic strength, $k_2^{(f\text{-}PC)}$ ($> 200 \times 10^6$ M^{-1} s^{-1}), for the reduction of plastocyanin by cytochrome *f*, and ~1/30 of $k_2^{(f\text{-}PC)}$ at the ionic strength estimated for the thylakoid interior. In contrast to $k_2^{(f\text{-}PC)}$, $k_2^{(ISP\text{-}f)}$ was independent of pH and ionic strength, implying no significant role of electrostatic interactions. Effective p*K* values of 6.2 and 8.3, respectively, of oxidized and reduced ISP were derived from the pH dependence of the amplitude of cytochrome *f* reduction. The first-order rate constant, $k_1^{(ISP\text{-}f)}$, predicted from $k_2^{(ISP\text{-}f)}$ is ~10 and ~150 times smaller than the millisecond and microsecond phases of cytochrome *f* reduction observed *in vivo*. It is proposed that in the absence of electrostatic guidance, a productive docking geometry for fast electron transfer is imposed by the guided trajectory of the ISP extrinsic domain. The requirement of a specific electrically neutral docking configuration for ISP electron transfer is consistent with structure data for the related cytochrome bc_1 complex.

The lumenal and intramembrane domains of the cytochrome b_6f complex of oxygenic photosynthesis contain four redox centers: cytochrome *f* with one covalently bound *c*-type heme, cytochrome *b* with two noncovalently bound *b*-type hemes, and one [2Fe-2S] cluster in the Rieske iron-sulfur protein (1–3). The electron transfer pathway, plastoquinol → Rieske ISP[1] → cytochrome *f* → plastocyanin or cytochrome c_6 → photosystem I on the lumen (*p*-side) of the membrane, comprises the high potential electron transport chain of the plastoquinol oxidase, whereas electron transfer between the two *b*-hemes, heme b_p → heme b_n, to a putative *n*-side bound quinone defines the low potential chain. Absorption of a photon and charge separation in photosystem I causes the oxidation of cytochrome *f* by plastocyanin ($t_{1/2} \approx 200$ μs, $k_1^{(f\text{-}PC)} \approx 3000$ s^{-1}) (4–7) after which the cytochrome is re-reduced by the Rieske iron-sulfur protein, which is usually poised in the reduced state in the dark, with half-time, $t_{1/2}$, ≈3–5 ms (first-order rate constant, $k_1^{(ISP\text{-}f)} \approx 250$–$150$ s^{-1}). Only about half of the chemical content of cytochrome *f* is observed to turn over with this half-time after a short, 5-μs flash (8–10). The other half has been inferred to be reduced too rapidly to be observed (10), with a rate constant, ~10^4 s^{-1}, presumably similar to the fast phase of reduction of cytochrome c_1 in the bc_1 complex (11).

Structure studies on the related cytochrome bc_1 complex from bovine and avian mitochondria showed the extrinsic domain of the ISP and the [2Fe-2S] cluster itself in well separated conformations, which depend on the crystal form and the presence of inhibitors bound to the complex (12, 13). The two extreme positions of the [2Fe-2S] cluster, separated by ~16 Å, are (i) proximal to the site (Q_p) of the bound ubiquinol inhibitor analogue, *e.g.* stigmatellin, and the cytochrome *b* polypeptide; and (ii) proximal to cytochrome c_1 via the heme propionate of the π-bonded heme (12). Neither of the individual conformations would allow the ISP to serve as both an electron acceptor for quinol oxidation and an electron donor to cytochrome c_1 (14). The net 16-Å translation of the [2Fe-2S] cluster occurs as a result of a rotation of the globular extrinsic domain by ~57° around an axis that includes the 9-residue peptide that links the globular extrinsic and transmembrane domains (12, 15–17). At least one additional stable intermediate position along this rotational trajectory has been defined (15). The inference that electron transfer mediated by the ISP in the cytochrome bc_1 complex occurs via its rotational-translational movement between donor and acceptor sites, dependent upon flexibility of the linker region, has been supported by mutation-function analysis of the linker peptide segment (16, 18, 19).

Given the homologies: (*a*) between the cytochrome b_6/subunit IV polypeptides and mitochondrial cytochrome *b* measured at low resolution (20), (*b*) the hydropathy and histidine ligation

* This work was supported by National Institutes of Health Grant GM-38323 and a Henry Koffler Professorship (to W. A. C.), USDA Grant 97-35306-455), National Science Foundation Grant MCB 0091415, and the University of Wisconsin, Oshkosh Faculty Development Fund (to T. K.). The costs of publication of this article were defrayed in part by the payment of page charges. This article must therefore be hereby marked "*advertisement*" in accordance with 18 U.S.C. Section 1734 solely to indicate this fact.

§ To whom correspondence may be addressed.
** Present address: Dept. of Pharmacology, University of Wisconsin, 1300 University Ave., Madison, WI 53706.

[1] The abbreviations used are: ISP, iron-sulfur protein; CHES, 2-(cyclohexylamino)ethanesulfonic acid; MES, β-morpholineethanesulfonic acid; PC, plastocyanin; PSI, photosystem one; *p*-side, electrochemically positive side of the membrane; Q_p, quinone binding site on the electrochemically positive side of the membrane; TRICINE, *N*-[2-hydroxy-1,1-bis(hydroxymethyl)ethyl]glycine; E_m, midpoint redox potential.

identities predicted from the respective gene sequences (21), (*c*) the cluster-binding domains of the Rieske ISP (22), and (*d*) in addition the flexible nature of the polyglycine putative linker region in the ISP of the b_6f complex (22), it is inferred that the ISP in the b_6f complex also carries out its electron transfer function by a large-scale rotation-translation between donor-acceptor sites. This inference is supported by orientation changes of the principal g values of the [2Fe-2S] system in the isolated b_6f complex induced by the *p*-side quinone analogue inhibitor, 2,5-dibromo-3-methyl-6-isopropylbenzoquinone (23) or metal ions (24), and the systematic effect of increased ambient viscosity on the rate of reduction of cytochromes *f* and b_6 in thylakoid membranes (25).

The 3–5-ms half-time for the reduction of cytochrome *f* by the Rieske ISP is the rate-limiting step of the b_6f complex, and of oxygenic photosynthesis. The events included in the observable reduction of cytochrome *f* include: (i) electron transfer from plastoquinol to the ISP; (ii) release of the ISP from the quinol-proximal binding site; (iii) tethered movement of the ISP from its quinol-proximal site to a site close to the cytochrome *f* heme, as described above; (iv) electron transfer from the docked ISP to cytochrome *f*.

Stopped-flow and equilibrium measurements were employed to follow the kinetics and pH dependence *in vitro* of the docking and electron transfer reaction of soluble redox-active fragments, 142 and 252 residues, respectively, of the Rieske ISP and cytochrome *f*. These data show that electron transfer in solution between these partners cannot rely on electrostatically guided docking, as occurs with plastocyanin/cytochrome *f*; the second-order rate constant obtained *in vitro* predicts a first-order rate constant *in vivo* that is substantially smaller than the observed values.

MATERIALS AND METHODS

Plasmid Construction—Plasmid pOSH37d was constructed to produce the 142-residue *Chlamydomonas reinhardtii* chloroplast Rieske iron-sulfur fragment, CRN37d (142 residues, deletion of 37 N-terminal residues). A segment of the *PetC* gene was amplified from *Chlamydomonas* RNA by reverse transcriptase-PCR and inserted into plasmid pET32a (Novagen, Madison, WI). This plasmid (pOSH37d or pTRXCRN37d) carries a fused open reading frame for thioredoxin, a 6-histidine tag for affinity purification, two thrombin cleavage sites, and the Rieske CRN37d ISP under control of a T7 RNA polymerase promoter.

Expression of the Truncated Fragment of the Rieske Iron-Sulfur Protein, Reconstitution of the 2Fe-2S Cluster, and Protein Purification—Procedures for *Chlamydomonas* ISP were based on those developed previously for cyanobacterial ISP.[2] *Escherichia coli* AD494(DE3) (Novagen) carrying pOSH37d was grown to early exponential phase (40–60 Klett units, Klett-Summerson colorimeter) in LB medium supplemented with 150 μg/ml ampicillin, 1 mM $FeSO_4$, and 2 mM cysteine typically at 25 °C. Isopropyl-β-D-thio-galactopyranoside was added to 0.1 mM and incubation was continued overnight. Harvested cells were suspended in 50 mM Tris-HCl buffer at pH 8.2. Urea was added to 8 M and the cells were broken by three passages through a French pressure cell at 20,000 p.s.i. and 4 °C. The ISP fusion protein in the crude supernatant fraction was reconstituted with iron-sulfur clusters as described in Refs. 26 and 27 but with the detergents and dialysis steps omitted. Fusion protein was purified directly from the reconstitution mixture (after dilution of urea to 0.8 M) by fast protein liquid chromatography (Amersham Biosciences) and either His-Bind (Novagen) or DEAE-Sepharose Fast Flow (Amersham Biosciences) resins. The latter, which sometimes gave cleaner separation, was used for the current work. The crude, reconstituted fusion protein preparation was loaded onto the column in 20 mM Tris-HCl, pH 8.3, buffer and eluted with a 0–1.0 M gradient of NaCl in the same buffer. The fusion protein, which eluted at about 300 mM NaCl, was concentrated by ultrafiltration (Amicon YM10 membrane) to several milligrams/ml and cleaved overnight with thrombin (0.2 units/mg of protein) at room temperature. Cleavage yielded a 13.9-kDa His-tagged thioredoxin fragment, a 3.9-kDa linker fragment, and the 14.9-kDa CRN37d ISP. The ISP was purified by passage over nickel-nitrilotriacetic acid His-Bind Superflow resin (Novagen) followed by diafiltration (YM-10 membrane) to a concentration of about 1.7 mg/ml (107 μM). The protein concentration of the ISP was estimated by its absorbance at 280 nm and predicted extinction coefficient of 3.17×10^4 M^{-1} cm^{-1} (28).

EPR Spectroscopy of the Rieske ISP—EPR spectra were obtained on a Varian E-4 X-band spectrometer as described previously (26) at ~15 K, 5 mW microwave power, 10 G modulation amplitude, 0.128-s time constant, and 100 KHz modulation frequency. ISP samples were found to be nearly fully reduced as prepared because the addition of ascorbate produced minimal increases in signal amplitude. The spin concentration of ISP [2Fe-2S] clusters was estimated by double integration of the EPR signal and comparison against a copper-perchlorate standard (29).

Expression of a Soluble Fragment of Cytochrome f in E. coli—A 252-residue redox-active fragment of wild type cytochrome *f* was overproduced in *E. coli* as described in Ref. 7. The cytochrome *f* construct was co-transformed with pEC86 that carries the cassette of cytochrome *c* maturation genes (30) into strain MV1190. The cells were grown semianaerobically at 37 °C for 20–24 h. The cells were harvested and broken by osmotic shock with 20% sucrose in 30 mM Tris-HCl, pH 7.5. Crude cytochrome *f* in the supernatant was passed through a DE-52 ion-exchange column. Fractions containing cytochrome *f* were then pooled, concentrated, and passed through a Sephadex G-100 size exclusion column. Cytochrome *f* fractions with $A_{554}/A_{280} > 0.7$ were then passed through a hydroxyapatite column; fractions with $A_{554}/A_{280} \geq 0.9$ were collected.

Purification of Plastocyanin from C. rienhardtii—Plastocyanin was isolated and purified from wild-type *C. reinhardtii* cells through ammonium sulfate precipitation as described in Ref. 6.

Reaction of ISP with Cytochrome f—The rate of reduction of oxidized soluble cytochrome *f* by the soluble ISP fragment from *C. reinhardtii* was determined by following changes in the cytochrome absorbance at 421 nm in a stopped-flow spectrophotometer (Applied Photophysics SX.18MV) at room temperature. Cytochrome *f* was oxidized by potassium ferricyanide and the excess oxidant was removed by filtration through a Centricon 10 filtration unit. Second-order rate constants were obtained from a set of pseudo-first order rate measurements, in which this rate was measured as a function of the concentration of cytochrome *f*, 10-, 15-, and 20-fold greater than that of the ISP. Conditions for which the concentration of ISP was in excess of that of cytochrome *f* yielded the same results. The reaction of oxidized cytochrome *f* and ISP under equilibrium conditions was carried out by mixing the two proteins and then scanning the spectrum of cytochrome *f* from 400 to 580 nm in a Cary 3 (Varian) spectrophotometer.

pH Titration of the Reaction of ISP and Cytochrome f—Equimolar concentrations (0.5 μM) of oxidized cytochrome *f* and reduced ISP were mixed and the spectrum of cytochrome *f* was scanned from 400 to 580 nm. The reaction was performed initially at pH 4.1; the pH was then increased incrementally (in steps of 0.5 pH units) to pH > 8.0 by adding microliter amounts of 5–10 M NaOH. The spectrum of cytochrome *f* at each pH was recorded in a Cary 3 spectrophotometer. The amount of cytochrome *f* reduced was calculated from the amplitude of the α (554 nm) difference band at each pH using an extinction coefficient of 2.6×10^4 M^{-1} cm^{-1} (31).

RESULTS

Overproduction and Purification of the Rieske ISP—The soluble fragment of the *Chlamydomonas* chloroplast Rieske protein was expressed in *E. coli* as a chimeric thioredoxin/Rieske ISP fusion protein and reconstituted *in vitro* with iron and sulfide to regenerate the 2Fe-2S cluster. SDS-PAGE of the purified fusion protein is shown (Fig. 1*A*). Thrombin cleavage, passage over nickel-nitrilotriacetic acid resin, and ultrafiltration generated the 14.9-kDa Rieske ISP (Fig. 1*B*). Restoration of typical Rieske 2Fe-2S clusters to the expressed ISP is demonstrated by the low temperature EPR spectrum ($g_x = 1.75$, $g_y = 1.90$, $g_z = 2.03$), characteristic of the high potential Rieske [2Fe-2S] protein (Fig. 1*C*). The 142-residue ISP (CRN37d) carries two residues (Gly and Ser) of the thrombin cleavage site in front of the flexible hinge region starting at residue Phe-38. Based on the estimation of protein concentration and spin quantification of the EPR signal, the cluster content of the reconstituted ISP was ~65%. The ascorbate-reduced minus ferricyanide-oxidized chemical difference spectrum for the ISP

[2] Y. S. Cho and T. Kallas, unpublished data.

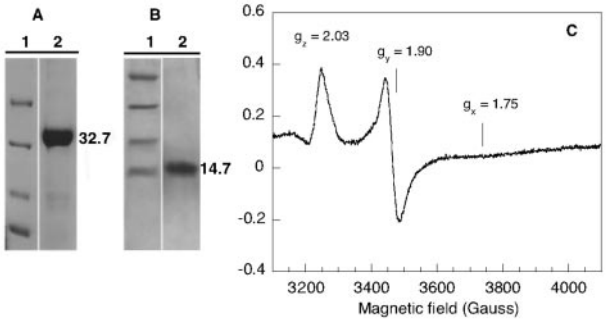

FIG. 1. **SDS-PAGE and EPR spectrum of the *Chlamydomonas* Rieske fragment.** *Panels A* and *B* display the SDS-PAGE of the overproduced, purified, and reconstituted TRXCRN37d fusion protein, and the Rieske ISP after thrombin cleavage and separation from the fusion protein. *Lanes 1* in both panels show molecular mass standards (14.4, 21.5, 31, and 45 kDa). *Panel C* shows an EPR spectrum of the purified and reduced ISP (protein concentration, 107 μM) obtained as described under "Materials and Methods." The characteristic g values of the Rieske 2Fe-2S cluster are shown.

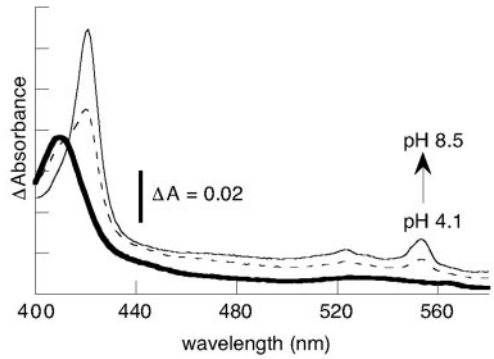

FIG. 2. **Reduction of cytochrome *f* by the Rieske ISP *in vitro*.** The *bold trace* is a spectrum of oxidized cytochrome *f* alone. The *thin solid* and *dashed traces* are spectra of cytochrome *f* after reaction with the Rieske ISP at pH 8.5 and 4.1, respectively. Reaction mixtures contained 0.5 μM reduced Rieske ISP, 0.5 μM oxidized cytochrome *f*, 0.5 mM EDTA, 10 mM each of succinate, MES, HEPES, TRICINE, and CHES buffers.

has broad positive and negative peaks at 400 and 476 nm (data not shown) with relatively weak extinction coefficients. This implies that: (*a*) the more narrow absorbance bands of cytochrome *f*, with much higher extinction coefficients, would be more useful for optical assay of electron transfer between the pair; and (*b*) the interference from ISP absorbance would be negligible (~0.4% in the presence of equimolar amounts of the two proteins) in the assay of cytochrome *f* reduction measured using the Soret band of the latter (Fig. 2).

In Vitro Reaction between C. reinhardtii ISP and Cytochrome f—The soluble ISP was able to transfer an electron to oxidized cytochrome *f*, as shown by the decrease in absorbance of cytochrome *f* at 410 nm and the increase in its absorbance at 421 nm (Fig. 2). The spectrum of oxidized cytochrome *f* is defined by a sharp Soret peak at 410 nm whereas its α band around 554 nm is featureless. The increase in amplitude of the Soret peak at 421 nm associated with its reduction by the ISP is accompanied by the appearance of a distinct α-band at 554 nm. Redox reactions of cytochrome *f* were observed by following changes in the Soret band at 410 or 421 nm, rather than the α-band whose extinction coefficient is ~⅛ that of the Soret band.

Stopped-flow measurements of the reaction between reduced Rieske ISP and oxidized cytochrome *f* yielded a second-order rate constant, $k_2^{(\text{ISP-f})} \approx 1.5 \times 10^6$ M^{-1} s^{-1}. Typical traces of the kinetics of cytochrome *f* reduction at pH 5.6 and 7.5 are shown in Fig 3*A* and summarized in Table I. Under the same reaction conditions, the rate of electron transfer from cytochrome *f* to PC is more rapid, with $k_2^{(\text{f-PC})} \sim 200 \times 10^6$ and 50×10^6 M^{-1} s^{-1}, respectively, at pH 7, and 0.01 and 0.2 M ionic strength (6, 32). No variation in the $k_2^{(\text{ISP-f})}$ was observed between ionic strengths of 0.01 and 0.10 M, nor between pH 7.5 and 5.6. Although there was no observable pH dependence for $k_2^{(\text{ISP-f})}$, the amplitude of cytochrome *f* reduction was larger at pH 7.5 than at 5.6 (Fig. 3*A*). The kinetics of cytochrome *f* reduction by ISP was also measured as a function of wavelength to generate a "stopped-flow spectrum" of the reaction (Fig. 3*B*). The stopped-flow spectrum peaks at 421 nm, and is virtually identical to the Soret band of the reduced minus oxidized chemical difference spectrum, indicating that the kinetics observed in the stopped-flow experiment were specifically those associated with cytochrome *f* reduction.

pH Titration of the Reaction of ISP and Cytochrome f—The E_m of cytochrome *f* is pH-independent between pH 4 and 8 (33), whereas the 139-residue ISP isolated from spinach chloroplasts has a pH-dependent E_m, $\Delta E_m(\text{pH}) = -30$ mV/pH (34). A larger pH dependence of the E_m, $\Delta E_m(\text{pH}) = -60$ mV/pH was obtained for the ISP [2Fe-2S] cluster in isolated cytochrome b_6f complexes from spinach (35). In either case, ΔE_m increases, and the amount of cytochrome *f* reduced by ISP in the reaction, ISP(red) + cytochrome *f*(ox) → ISP(ox) + cytochrome *f*(red), increases with increasing pH (Figs. 2 and 4*A*). A plot of the amplitude of cytochrome *f* reduced by an equimolar quantity of ISP (Fig. 4*A*) reflects the pH dependence of the E_m of the ISP (34, 35). The pH dependence of the extent of cytochrome *f* reduction by the ISP at each pH was identical when measured in the α- and Soret bands of cytochrome *f*. Cytochrome *f* is ~50

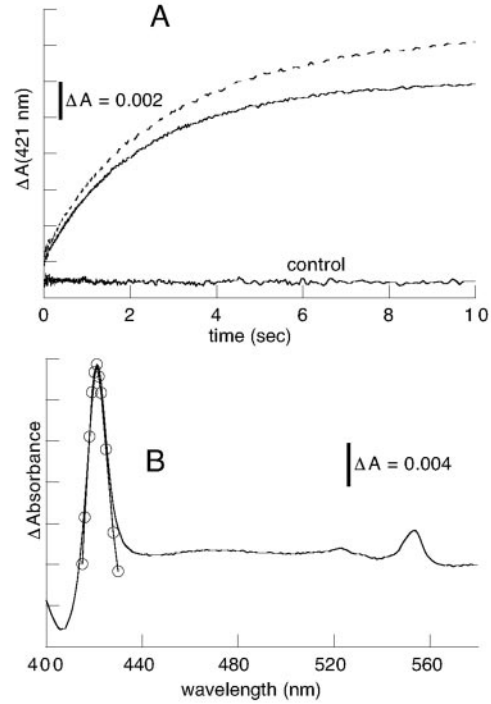

FIG. 3. **Kinetics of cytochrome *f* reduction by the Rieske ISP *in vitro*.** *A*, reactions were performed at pH 5.6 (*solid line*) and pH 7.5 (*dashed line*) at room temperature in a stopped-flow spectrophotometer (see "Materials and Methods"). Cytochrome *f* reduction was monitored by absorbance changes at 421 nm. The "control" trace contained only buffer and oxidized cytochrome *f*. *B*, stopped-flow spectrum (*open circles*) of the cytochrome *f*/ISP reaction, obtained by following the reaction kinetics at several wavelengths around 421 nm, superimposed on the chemical difference spectrum of reduced-oxidized cytochrome *f*. Reaction mixtures contained 0.25 μM reduced ISP, 0.25 μM oxidized cytochrome *f*, 0.5 mM EDTA, and 10 mM HEPES-NaOH at pH 5.6 or 7.5.

TABLE I
Rate constants for oxidation of the Rieske iron-sulfur protein and oxidation-reduction of cytochrome (cyt) f

In vivo,[a] k_1 (s^{-1})		*In vitro,*[b] k_2 ((M^{-1} s^{-1}) × 10^{-6})			*In vitro,*[c] k_1 (s^{-1})
ISP → Cyt *f*	Cyt *f* → PC	I(M)[d]	ISP[b] → Cyt *f*	Cyt *f* → PC	ISP → Cyt c_1
150–250	~2,400–3,000[e]	0.01	~1.5	>200	16,000 (2/3),[c] 250 (1/3)
		0.20	~1.5	50	

[a] Rate constants obtained for cytochrome *f* oxidation-reduction in chloroplasts or cells of *C. reinhardtii* (4, 5, 7).
[b] Rate constants obtained from stopped-flow data in the present study.
[c] Rate constants were obtained from measurements in isolated cytochrome bc_1 complexes; 2/3 and 1/3 of the amplitude of the cytochrome c_1 reduction is associated with the large and small rate constants (11).
[d] I(M), ionic strength.
[e] Rate constant determined from *in vitro* reaction of cytochrome *f* and PC initiated by flash photolysis of flavin-semiquinone (32, 47).

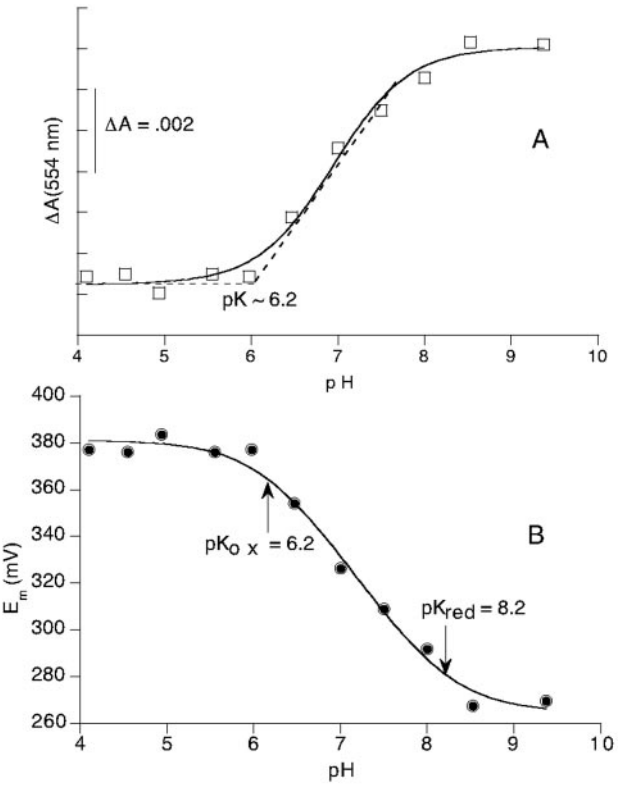

FIG. 4. **pH dependence of the reaction between oxidized cytochrome *f* and reduced Rieske ISP.** *A*, amplitude of cytochrome *f* reduction by the ISP as a function of pH, shown as the amplitude of the α-band, 554 nm, of reduced cytochrome *f*. The reaction was initially at pH 4.1; pH values were adjusted as described under "Materials and Methods." *B*, pH dependence of the E_m of the ISP. The E_m at each pH was obtained from the data in *A* and the known E_m of cytochrome *f* that is constant at ~370 mV from pH 4 to 8.5. The *solid line* is a fit to $E_m = E_{m,\text{low pH}} - 59\ \log((K_{ox} + H^+)/(K_{red} + H^+))$ with pK_{ox} = 6.2 and pK_{red} = 8.3. The reaction mixture contained: 0.5 μM reduced ISP, 0.5 μM oxidized cytochrome *f*, 0.5 mM EDTA, 10 mM each of succinate, MES, HEPES, TRICINE, and CHES buffers.

and ~95% reduced at pH 4.1 and 8.5, respectively, as seen by the amplitude of the α- and Soret band peaks (Figs. 2 and 4*A*). The pK_{ox} for the reaction is ~6.2, which is close to the value previously measured by titration of the visible spectrum of the 139-residue ISP isolated from the spinach b_6f complex (34), but lower than the p*K* values of 7.6–7.8 determined for the ISP of the b_6f complex by EPR at cryogenic temperature (35).

pH Dependence of the Midpoint Potential of the ISP—The midpoint potential of the ISP at each pH point in Fig. 4*B* could be determined from the known amount of oxidized and reduced cytochrome *f*, and from the known midpoint potential of cytochrome *f* (E_m = +370 mV), which is pH-independent from pH 4 to 8. A plot of E_m *versus* pH for the ISP is shown (Fig. 4*B*). p*K* values of 6.2 and 8.2 for the oxidized and reduced forms, respectively, of the ISP were obtained by least squares fit to the formula, $E_m = E_{m,\text{low pH}} - 59\ \log((K_{ox} + H^+)/(K_{red} + H^+))$, where K_{ox} and K_{red} are acid dissociation equilibrium constants for the oxidized and reduced species, respectively. Although two p*K* values of 7.6 and 9.2 were inferred for the oxidized form of the ISP from bovine heart mitochondria (36), the fit to the present data does not require a fit to two p*K* values.

The slope of the curve in the pH-dependent region from pH 6 to 8.5 is −40 mV/pH, in agreement with the approximately −30 mV/pH obtained from optical titration in the visible spectrum (34), but smaller than the −80 mV/pH obtained for isolated *bf* complexes by EPR titration of the midpoint potential (35). Titration of the pH dependence of the E_m of the ISP from cytochrome *bc* complexes, using the weak 500-nm band of the circular dichroism spectrum, yielded slopes of about −120 mV/pH at pH > 8 and −60 mV/pH below pH 8 (36, 37).

DISCUSSION

Does the $k_2^{(ISP\text{-}f)}$ Measured in Vitro Account for the Observed Rate of Cytochrome f Reduction in Situ and in Vivo?—To calculate the first-order rate constant *in vivo*, $k_1^{(ISP\text{-}f)}$, from the second-order rate constant, $k_2^{(ISP\text{-}f)}$, one must estimate the intramembrane concentration of the ISP as follows: (i) $k_2^{(f\text{-}PC)}$ in the 0.2 M solution environment estimated for the thylakoid lumen (38) is 50×10^{-6} M^{-1} s^{-1} (6); (ii) the observed first-order rate constant $k_2^{(f\text{-}PC)}$~ 2500–4000 s^{-1} implies a lumenal PC concentration of 6×10^{-5} M. If there are 4 PC per cytochrome *f* (or ISP) (39), then the ISP concentration *in vivo* is ≈1.5×10^{-5} M. Using the measured $k_2^{(ISP\text{-}f)}$ of 1.5×10^{-6} M^{-1} s^{-1}, an *in vivo* first-order rate constant of cytochrome *f* reduction, $k_1^{(ISP\text{-}f)}$, of 20 s^{-1} is obtained. This value of $k_1^{(ISP\text{-}f)}$ calculated from $k_2^{(ISP\text{-}f)}$ is smaller than the observed $k_1^{(ISP\text{-}f)} \approx 150\text{–}250$ s^{-1} for the slow phase of cytochrome *f* reduction. An additional rate constant that includes a microsecond rate of cytochrome *f* reduction is required to describe the reduction kinetics of the total complement of cytochrome *f* *in situ* or *in vivo*.

The Two Kinetic Components of Cytochrome f Reduction in Situ and in Vivo—The ISP and cytochrome *f* components of the high-potential (E_m > 0.3 V) chain of the cytochrome b_6f complex are initially reduced before oxidation of PSI by a short (microsecond) light flash. This results in an observable oxidation of ~50% (1:1600 chlorophyll) of the total chemical content of cytochrome *f* (1:800 chlorophyll) via plastocyanin with a $k_1^{(f\text{-}PC)} \sim 2700$ s^{-1} (Fig. 5*A*), and reduction with $k_{1,slow}^{(ISP\text{-}f)} \approx 150\text{–}250$ s^{-1}. The missing 50% of the amplitude of cytochrome *f* oxidation-reduction can be accounted for if an additional microsecond kinetic component, $k_{1,fast}^{(ISP\text{-}f)}$, similar to that observed in the reduction of cytochrome c_1 (11), is included in describing the reduction of cytochrome *f* (Fig. 5*A*). The kinetics of cytochrome *f* oxidation-reduction can be described as the change in absorbance, $\Delta A(t)$, according to: $\Delta A(t) = \Delta A_{max}[(1 - \exp(-k_1^{(f\text{-}PC)} \cdot t))(0.5\exp(-k_{1,fast}^{(ISP\text{-}f)} \cdot t) + 0.5\exp(-k_{1,slow}^{(ISP\text{-}f)} \cdot t]$, where $k_1^{(f\text{-}PC)}$ is the first-order rate constant for cytchrome *f* oxidation, $k_{1,fast}^{(ISP\text{-}f)}$ and $k_{1,slow}^{(ISP\text{-}f)}$ are rate constants for cytochrome *f* reduction, and ΔA_{max} is the total change in absorbance associated with full oxidation of cytochrome *f*. As shown in Fig. 5*A*, rapid

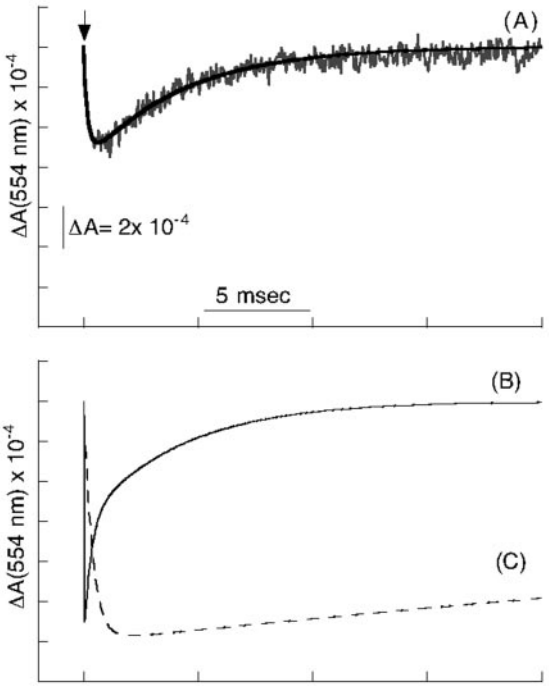

FIG. 5. **Time course of light-induced cytochrome *f* oxidation-reduction in chloroplast thylakoids.** *A*, superimposed on the experimental trace (*gray*) is a simulation of cytochrome *f* oxidation-reduction kinetics using $\Delta A(t) = \Delta A_{max}[(1 - \exp(-k_1^{(f\text{-}PC)} \cdot t))(0.5\exp(-k_{1,fast}^{(ISP\text{-}f)} \cdot t) + 0.5\exp(-k_{1,slow}^{(ISP\text{-}f)} \cdot t)]$; $k_1^{(f\text{-}PC)} = 2700\ s^{-1}$, $k_{1,fast}^{(ISP\text{-}f)} = 3200\ s^{-1}$, $k_{1,slow}^{(ISP\text{-}f)} = 240\ s^{-1}$, $\Delta A_{max} = 12 \times 10^{-4}$. ΔA_{max} corresponds to oxidation of the total chemical content of cytochrome *f*. The *arrow* indicates start of the light flash. According to the simulations, the full ΔA_{max} is observed if: *B*, $k_1^{(f\text{-}PC)}$ is very large, $\sim 10^5\ s^{-1}$, or *C*, $k_{1,fast}^{(ISP\text{-}f)} = 0$ and $k_{1,slow}^{(ISP\text{-}f)}$ is very small, $\sim 10\ s^{-1}$. The ΔA scale in *A* applies also to *B* and *C*.

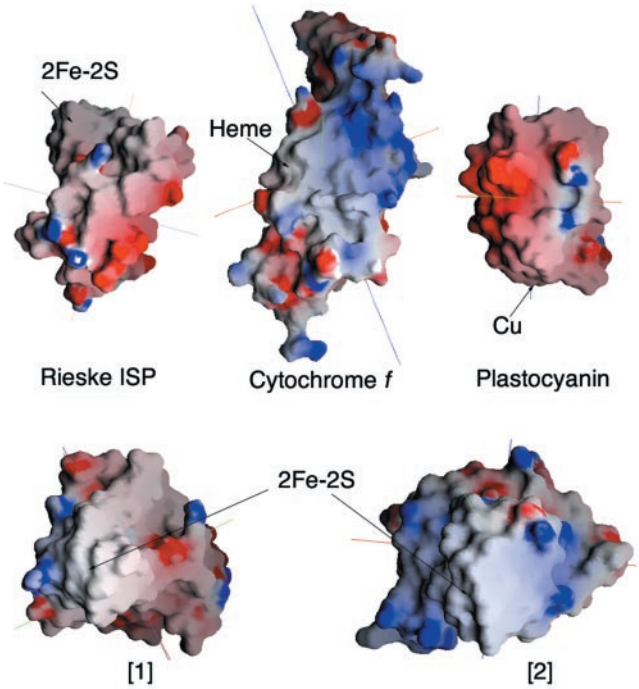

FIG. 6. **Surface potentials of Rieske ISP, cytochrome *f*, and plastocyanin calculated with the program GRASP (48).** The potentials range from +10 kT (*blue*) to −10 kT (*red*); *kT*, thermal energy, 25 mV. *Top*, the structures for the soluble domains of spinach ISP and *C. reinhardtii* cytochrome *f*, and for plastocyanin (49, 50), were used in the calculation. *Bottom*, comparison of the surface potentials around the [2Fe-2S] cluster of *1*, spinach ISP, and *2*, bovine ISP. The charged residues are Lys, Arg, Glu, and Asp.

re-reduction of 50% of the cytochrome *f* prevents observation of the full oxidation of the total chemical content of cytochrome *f,* in this case $k_1^{(f\text{-}PC)} = 2700\ s^{-1}$ and $k_{1,fast}^{(ISP\text{-}f)} = 3200\ s^{-1}$. To observe full oxidation, the rate of cytochrome *f* oxidation should be much faster (Fig. 5*B*), or its rate of reduction, $k_{1,slow}^{(ISP\text{-}f)}$, much slower (Fig. 5*C*) than the observed rates.

ISP and Plastocyanin Utilize Different Mechanisms to Dock to Cytochrome f—The slow electron transfer between ISP and cytochrome *f* in solution that is independent of pH and ionic strength shows that the ISP and cytochrome *f* are not able to find a competent docking site through electrostatic guidance in solution. Considering the regions of prominent electrostatic potential on the surfaces of plastocyanin and the soluble domains of cytochrome *f* and the ISP (Fig. 6, *top*), it is expected that ISP, like plastocyanin, would be able to utilize electrostatic guidance. However, the prominent negative patch on the surface of the ISP lies away from the cluster so that even if electrostatic interactions are utilized to dock the proteins, the resulting complex would be unproductive.

Hypotheses to Explain the Small $k_2^{(ISP\text{-}f)}$—The second-order rate constant *in vitro*, $k_2^{(ISP\text{-}f)} = 1.5 \times 10^6\ M^{-1}\ s^{-1}$ predicts a rate constant for cytochrome *f* reduction that is slower than the observed $k_{1,slow}^{(ISP\text{-}f)} = 240\ s^{-1}$ and $k_{1,fast}^{(ISP\text{-}f)} = 3200\ s^{-1}$ by ~10 and 150×, respectively. There are two obvious hypotheses that can explain the small value of $k_2^{(ISP\text{-}f)}$ that is ineffective at docking *in vitro* between ISP and cytochrome *f*: (i) alteration or damage to the soluble cytochrome *f* or ISP fragments. The possibility of small but critical structural changes cannot be excluded. However, the soluble ISP has a normal EPR spectrum (Fig. 1*C*) and E_m, the latter assayed from the extent of reduction of cytochrome *f* at equilibrium (Figs. 2 and 4, *A* and *B*). The soluble 252-residue cytochrome *f* has a normal optical spectrum and E_m (7), and rapidly transfers electrons to PC with kinetics that are dependent upon ionic strength and the presence of specific basic residues. (ii) Docking and electron transfer *in vitro* are inefficient because of the absence of electrostatic or structural guidance. It is inferred that the flexible membrane-embedded ISP tether provides constraints that assure formation of a docked configuration of the ISP-cytochrome *f* complex that allows more efficient electron transfer.

It can be seen that the mitochondrial ISP uses the same surface domain to dock in proximity to (i) the cytochrome c_1 heme (Fig. 7, *A* and *B*), and (ii) the quinol Q_p (or quinone analogue inhibitor) binding site (Fig. 7*C*). The active face of the ISP around the [2Fe-2S] cluster is electrically neutral in both the bc_1 (15) and b_6f (22) complexes (Fig. 6, *bottom*). The absence of any electrostatic influence on the interaction between the ISP and cytochrome *f in vitro* implies that a specific electrically neutral docking geometry may be required for fast ISP-cytochrome *f* electron transfer. The use of the productive docking configuration, without wasteful searching of coordinate space for unproductive docking geometries, is imposed by the guided trajectory of the [2Fe-2S] cluster in the extrinsic domain of the ISP, which rotates about the flexible interfacial linker region (16).

pK_{ox} and E_m—The pK_{ox} = 6.2–6.5 of the isolated ISP from *C. reinhardtii* (Fig. 4*B,* above), or from spinach chloroplasts determined by room temperature optical difference spectra (34), is significantly more acidic than that (7.6–7.9) determined for the Rieske protein or a similar ISP from the *bc* complex in mitochondria and bacterial photosynthesis (>7.0). On the one hand, the difference of 1–1.5 pH units between the pK_{ox} value of the chloroplast (ambient pH ~ 6) (40) and mitochondrial/bacterial (ambient pH ~ 7.0) ISP agrees with the pH difference between the ambient environments in the two membrane systems, and the requirement that the ISP be able to cycle be-

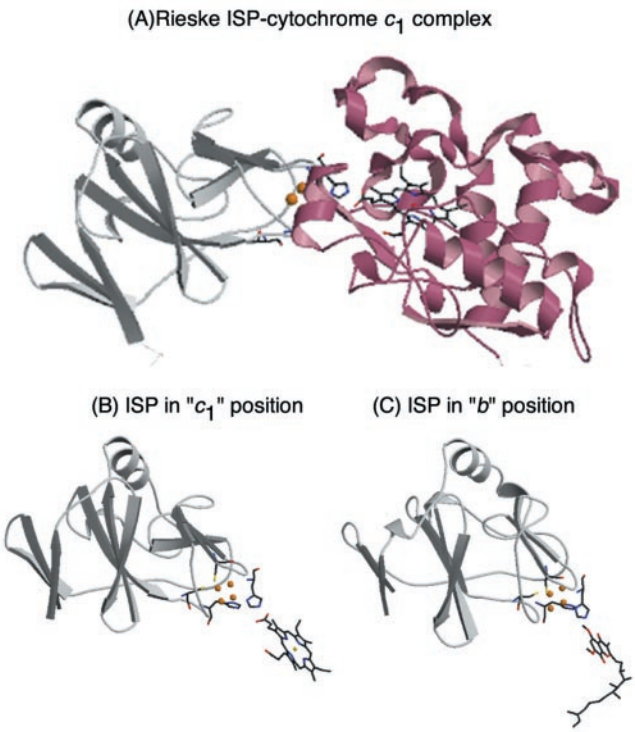

FIG. 7. **Docking of Rieske ISP and cytochrome c_1.** *A*, ISP is shown docked to cytochrome c_1 in the bovine mitochondrial cytochrome bc_1 complex (15). ISP is shown in its 2 extreme positions: *B*, proximal to cytochrome c_1 (15), and *C*, proximal to the Q_p-site ("*b*" position) (12). The [2Fe-2S] cluster of the ISP is shown as *orange spheres*. The figures were drawn with MOLSCRIPT (51) and rendered with Raster3D (52).

tween protonated and deprotonated states. For the latter purpose, the pK_{ox} should be close to the value of the ambient pH. The p*K* of the ISP is critical for charge-transfer reactions in the *bc* or *bf* complexes. (i) The bifurcated transfer of electrons from quinol to the ISP and to the low potential cytochrome *b* is believed to be initiated by deprotonation of quinol at the Q_p site. Quinol deprotonation has been proposed to occur via one of the histidine ligands of the 2Fe-2S because, as shown by the structure of the mitochondrial cytochrome *bc* complex, one of the oxygens of stigmatellin is within H-bonding distance to His-161 of the ISP (12, 13). If the first H^+ from quinol is indeed transferred to one of the histidine ligands of the ISP, this histidine should have a different protonation state depending on the redox state of the ISP. The values of pK_{ox} = 6.2 and pK_{red} = 8.3 determined *in vitro* raise a question about the protonation state of the ISP *in vivo*. At neutral pH, about 14% of the oxidized protein, or 95% of the reduced protein would be protonated. However, the pH in the lumen is acidic, with a pH estimated to be in the range of 5.8–6.5 (40). The reduced ISP is more than 95% protonated in this pH range, whereas the oxidized protein is about 30% protonated at pH 6.5. This consideration implies that the ISP is deprotonated only after it has been oxidized by cytochrome *f*.

These results for the pK_{ox} of the ISP of the b_6f complex are complicated by the finding that the pK_{ox} of the chloroplast ISP was >7.0 when it was measured by titration of its g_y EPR signal at 17 K. Furthermore, the pK_{ox} for the ISP in the intact b_6f complex determined by low temperature EPR was 7.6–7.8 (35). Some difference in structure between the native Rieske protein and the ISP, affecting the location relative to the [2Fe-2S] cluster of charged residues or dipole elements, is indicated by the limiting E_m of the ISP at acid pH being 50 mV more positive than that of native ISP (34).

Rate-determining Step for Charge Transfer through the Cytochrome b_6f Complex—The pH dependence of the rates of reduction of cytochromes *b* and *f* in the cytochrome *bf* complex (41, 42), and kinetic isotope effects (43), suggest the possibility of a rate-limitation because of proton-coupled electron transfer (7). From the observed decrease in turnover rate in site-directed mutants of the ISP of the cytochrome bc_1 complex that associated with a decreased ISP E_m (44, 45), it was inferred that the quinol-ISP electron transfer step is rate-limiting in the bc_1 complex. A slow phase of cytochrome c_1 reduction, $k_2^{(c1\text{-}ISP)}$ = 250 to 180 s^{-1} and 1000 s^{-1}, respectively, observed in photoactivated electron transfer using isolated mitochondrial and bacterial bc_1 complexes, was attributed to the quinol-ISP electron transfer step (11). The fast phase of the photoactivated cytochrome c_1 reduction, $k_{ET}^{(c1\text{-}ISP)} \sim$ 16,000–60,000 s^{-1} (11), was associated with electron transfer from ISP docked to cytochrome c_1, implying that electron transfer from docked ISP to cytochrome c_1 or *f* (see above) is also not rate-limiting.

The constrained and guided motion of the ISP can be considered as a candidate for the rate-limiting step. In the case of the bc_1 complex, it has been argued that the ISP motion is not rate-limiting (19). This is also implied by the identical rates of reduction of cytochrome c_1 and *b* in the photoactivated mitochondrial bc_1 complex (11). However, in the cytochrome b_6f complex, the slow phase of reduction of cytochromes *f* and b_6 were shown to be inversely proportional to the ambient lumenal viscosity, implying that the tethered motion of the ISP is rate-limiting (25).

Regulation and Control of ISP Rotation—The existence of the reversible rotational motion of the ISP in cytochrome *bc* complexes is presumably under control of redox events in the complex, and may involve interaction of the monomeric units of the dimeric complex (46). The fact that the observed turnover of cytochrome *f* involves ~50% fast and ~50% slow phases suggests a state of the b_6f complex in which ISP is bound to cytochrome *f* in one monomer of the complex and bound to the quinol-proximal site in the other. However, details of the regulation/control mechanism are obscure at present.

Acknowledgments—We thank D. Reardon (University of Wisconsin, Oshkosh, WI) for participation in the Rieske ISP expression work and W. Antholine and the National Biomedical ESR Center, Medical College of Wisconsin, for assistance with the ESR spectroscopy.

REFERENCES

1. Kallas, T. (1994) in *The Molecular Biology of Cyanobacteria* (Bryant, D. A., ed) pp. 259–317, Kluwer Academic Publishers, Dordrecht
2. Hauska, G., Schütz, M., and Büttner, M. (1996) in *Oxygenic Photosynthesis: The Light Reactions* (Ort, D. R., and Yocum, C. F., eds) Kluwer Academic Publisher, Amsterdam
3. Cramer, W. A., Soriano, G. M., Ponomarev, M., Huang, D., Zhang, H., Martinez, S. E., and Smith, J. L. (1996) *Annu. Rev. Plant Physiol. Plant Mol. Biol.* **47,** 477–508
4. Delosme, R. (1991) *Photosynth. Res.* **29,** 45–54
5. Soriano, G. M., Ponamarev, M. V., Tae, G.-S., and Cramer, W. A. (1996) *Biochemistry* **35,** 14590–14598
6. Soriano, G. M., Ponamarev, M. V., Piskorowski, R. A., and Cramer, W. A. (1998) *Biochemistry* **37,** 15120–15128
7. Ponamarev, M. V., and Cramer, W. A. (1998) *Biochemistry* **37,** 17199–17208
8. Whitmarsh, J., and Cramer, W. A. (1979) *Biophys. J.* **26,** 223–234
9. Jones, R. W., and Whitmarsh, J. (1988) *Biochim. Biophys. Acta* **933,** 258–268
10. Whitmarsh, J., Bowyer, J. R., and Crofts, A. R. (1982) *Biochim. Biophys. Acta* **682,** 404–412
11. Sadoski, R. C., Engstrom, G., Tian, H., Zhang, L., Yu, C. A., Yu, L., Durham, B., and Millett, F. (2000) *Biochemistry* **39,** 4231–4236
12. Zhang, Z., Huang, L., Shulmeister, V. M., Chi, Y. I., Kim, K. K., Hung, L. W., Crofts, A. R., Berry, E. A., and Kim, S. H. (1998) *Nature* **392,** 677–684
13. Hunte, C., Koepke, J., Lange, C., Robmanith, T., and Michel, H. (2000) *Structure* **8,** 669–684
14. Crofts, A. R., and Berry, E. A. (1998) *Curr. Opin. Struct. Biol.* **8,** 501–509
15. Iwata, S., Lee, J. W., Okada, K., Lee, J. K., Iwata, M., Rasmussen, B., Link, T. A., Ramaswamy, S., and Jap, B. K. (1998) *Science* **281,** 64–71
16. Izrailev, S., Crofts, A. R., Berry, E. A., and Schulten, K. (1999) *Biophys. J.* **77,** 1753–1768
17. Kim, H., Xia, D., Yu, C. A., Xia, J. Z., Kachurin, A. M., Zhang, L., Yu, L., and Deisenhofer, J. (1998) *Proc. Natl. Acad. Sci. U. S. A.* **95,** 8026–8033
18. Tian, H., Yu, L., Mather, M. W., and Yu, C.-A. (1998) *J. Biol. Chem.* **273,** 27953–27959
19. Darrouzet, E., Valkova-Valchanova, M., and Daldal, F. (2000) *Biochemistry* **39,**

15475–15483
20. Bron, P., Lacapere, J. J., Breyton, C., and Mosser, G. (1999) *J. Mol. Biol.* **287,** 117–126
21. Widger, W. R., Cramer, W. A., Herrmann, R. G., and Trebst, A. (1984) *Proc. Natl. Acad. Sci. U. S. A.* **81,** 674–678
22. Carrell, C. J., Zhang, H., Cramer, W. A., and Smith, J. L. (1997) *Structure* **5,** 1613–1625
23. Schoepp, B., Brugna, M., Riedel, A., Nitschke, W., and Kramer, D. M. (1999) *FEBS Lett.* **450,** 245–250
24. Roberts, A. G., Bowman, M. K., and Kramer, D. M. (2002) *Biochemistry* **41,** 4070–4079
25. Heimann, S., Ponamarev, M. V., and Cramer, W. A. (2000) *Biochemistry* **39,** 2692–2699
26. Holton, B., Wu, X., Tsapin, A. L., Kramer, D. M., Malkin, R., and Kallas, T. (1996) *Biochemistry* **35,** 15485–15493
27. Cheng, H., Westler, W. M., Xia, B., Oh, B.-H., and Markley, J. L. (1995) *Arch. Biochem. Biophys.* **316,** 619–634
28. Gross, R., Pytte, A., Green, D., and Doyle, J. (1999) *Gene Inspector, Sequence Analysis Computer Program,* Version 1.5, Textco, W. Lebanon, NH
29. Aasa, R., Albracht, P. J., Falk, K. E., Lanne, B., and Vanngard, T. (1976) *Biochim. Biophys. Acta* **422,** 260–272
30. Thöny-Meyer, L., Fischer, F., Kunzler, P., Ritz, D., and Hennecke, H. (1995) *J. Bacteriol.* **177,** 4321–4326
31. Metzger, S. U., Cramer, W. A., and Whitmarsh, J. (1997) *Biochim. Biophys. Acta* **1319,** 233–241
32. Qin, L., and Kostic, N. (1992) *Biochemistry* **31,** 5145–5150
33. Martinez, S., Huang, D., Ponamarev, M., Cramer, W. A., and Smith, J. L. (1996) *Protein Sci.* **5,** 1081–1092
34. Zhang, H., Carrell, C. J., Huang, D., Sled, V., Ohnishi, T., Smith, J. L., and Cramer, W. A. (1996) *J. Biol. Chem.* **271,** 31360–31366
35. Nitschke, W., Joliot, P., Liebl, U., Rutherford, A. W., Hauska, G., Miller, A., and Riedel, A. (1992) *Biochim. Biophys. Acta* **1102,** 266–268
36. Link, T. A., Hagen, W. R., Pierik, A. J., Assmann, C., and von Jagow, G. (1992) *Eur. J. Biochem.* **208,** 685–691
37. Ugulava, N. B., and Crofts, A. R. (1998) *FEBS Lett.* **440,** 409–413
38. Kaiser, W. M., Weber, H., and Sauer, M. (1983) *Z. Pflanzenphys.* **113,** 15–27
39. Haehnel, W., Ratajczak, R., and Robenek, H. (1989) *J. Cell Biol.* **108,** 1397–1405
40. Kramer, D. M., Sacksteder, C. A., and Cruz, J. A. (1999) *Photosynth. Res.* **60,** 151–163
41. Bendall, D. S. (1982) *Biochim. Biophys. Acta* **683,** 119–151
42. Hurt, E. C., and Hauska, G. (1981) *Eur. J. Biochem.* **117,** 591–599
43. Soriano, G. M., and Cramer, W. A. (2001) *Biochemistry* **40,** 15109–15116
44. Denke, E., Merbitz-Zahradnik, T., Hatzfeld, O. M., Snyder, C. H., Link, T. A., and Trumpower, B. L. (1998) *J. Biol. Chem.* **273,** 9085–9093
45. Crofts, A. R., Guergova-Kuras, M., Huang, L., Kuras, R., Zhang, Z., and Berry, E. (1999) *Biochemistry* **38,**
46. Gutierrez-Cirlos, E. B., and Trumpower, B. L. (2002) *J. Biol. Chem.* **277,** 1195–1202
47. Meyer, T. E., Zhao, Z. G., Cusanovich, M. A., and Tollin, G. (1993) *Biochemistry* **32,** 4552–4559
48. Nicholls, A., Sharp, K., and Honig, B. (1991) *Proteins* **11,** 281–296
49. Sainz, G., Carrell, C. J., Ponamarev, M. V., Soriano, G. M., Cramer, W. A., and Smith, J. L. (2000) *Biochemistry* **39,** 9164–9173
50. Redinbo, M., Cascio, D., Choukair, M. K., Rice, D., Merchant, S., and Yeates, T. O. (1993) *Biochemistry* **32,** 10560–10567
51. Kraulis, P. J. (1991) *J. Appl. Crystallogr.* **24,** 946–950
52. Merritt, E. A., and Murphy, M. E. P. (1994) *Acta Crystallogr. Sect. D* **50,** 869–873